Tuning the metal-insulator transitions of $(SrMnO_3)_n/(LaMnO_3)_{2n}$ superlattices: Role of interfaces

C. Adamo,[1] C. A. Perroni,[2] V. Cataudella,[2] G. De Filippis,[2] P. Orgiani,[3] and L. Maritato[3]
[1]*Department of Materials Science and Engineering, Cornell University, Ithaca, New York 14835-1501, USA*
[2]*Dipartimento di Scienze Fisiche and CNR-INFM Coherentia, Universitá di Napoli "Federico II", 80126 Napoli, Italy*
[3]*Dipartimento di Matematica ed Informatica and CNR-INFM Coherentia, Universitá di Salerno, 84081 Baronissi (SA), Italy*
(Received 15 December 2008; published 28 January 2009)

The temperature dependence of the transport properties of $(SrMnO_3)_n/(LaMnO_3)_{2n}$ superlattices has been systematically investigated by changing the number of interfaces while keeping the total thickness of the system fixed. The superlattices undergo a rich variety of transitions among metal, Mott variable range hopping insulator, interaction-induced Efros-Shklovskii insulator, and polaronic insulator. Interfaces play a fundamental role in tuning the metal-insulator transitions controlling the effective doping of the different layers. In the case of a bilayer, as clarified by a theoretical model, the single interface can extend its effects well far from it in the bulk layer.

DOI: 10.1103/PhysRevB.79.045125 PACS number(s): 75.47.Lx, 72.10.Di, 73.21.Cd, 73.40.−c

I. INTRODUCTION

Interfaces can drastically modify the electronic properties of correlated electron materials. Recent examples include the formation of a thin metallic layer at the interface between band and Mott insulators as, for example, between $SrTiO_3$ and $LaTiO_3$ (Refs. 1 and 2) or between the band insulators $LaAlO_3$ and $SrTiO_3$.[3] It has been also shown that metallicity and ferromagnetism can be induced at the interface between the antiferromagnetic insulating manganites $LaMnO_3$ (LMO) $[(Mn^{3+},t_{2g})^3e_g]$ and $SrMnO_3$ (SMO) $[(Mn^{4+},t_{2g})^3]$.[4]

In this framework magnetic and transport properties of $(SMO)_n/(LMO)_m$ superlattices (SLs) with several hole dopings $c=n/(m+n)$ in the range $0.2<c<0.5$ have been studied.[5,6] The behavior of these SL ranges from insulating to metallic depending on the value of c and the thickness of the LMO and SMO layers. In contrast to the A-site alloy $La_{1-x}Sr_xMnO_3$, within the SL, La^{3+} and Sr^{2+} ions are mostly separated by interfaces. Therefore, a sizable source of disorder is strongly reduced, opening the possibility of studying several phenomena that are not accessible in the less clean $La_{1-x}Sr_xMnO_3$ alloys.

In this work we have systematically investigated the temperature dependence of the transport properties of $(SMO)_n/(LMO)_{2n}$ SL $(c=1/3)$ with different values of n $(n=1, 2, 3, 4, 5, 6, 8,$ and $16)$. Here n denotes the number of pseudocubic unit cells comprising the thickness of each SMO layer in the SL. Due to the very low spatial disorder of our samples, we observe several transitions from metal to insulator as a function of n and temperature. Moreover, in the insulating regions, we identify clear crossovers from variable range hopping to polaronic insulators and from interaction-induced Efros-Shklovskii to variable range hopping behavior depending on temperature. Such a variety of transport regimes, observed at very different dopings in an A-site alloy, can be tuned changing only the interface number. The analysis of our data in comparison with a simple proposed model allows us to point out the fundamental role played by interfaces in clean layered systems. This effect is relevant even in the case of a single interface. In this case an electronic reconstruction nucleates at the interface and has an effect well far from it (about 30 unit cells in the case of the single interface LMO/SMO bilayer). A schematic sketch which summarizes the observed transport regimes is proposed in Fig. 1.

II. STRUCTURAL PROPERTIES AND FABRICATION DETAILS OF THE SL

$(SMO)_n/(LMO)_{2n}$ SL with long-range structural coherence was fabricated by molecular-beam epitaxy using layer-by-layer deposition on treated (100) $SrTiO_3$ substrates.[6] The films were all around 20 nm thick. The case $n=16$ corresponds to a SMO/LMO bilayer. Electronic transport measurements were performed by standard four-probe methods over the temperature range from 4 to 600 K. The high structural quality of our SL is revealed by x-ray measurements exhibiting all expected satellite reflections for the SL.[6] The systems also exhibit a low level of defects as suggested by the transport measurements. For $n=1$, in fact, the low-temperature resistivity increases as T^α with $\alpha\simeq 2.5$, and the residual resistivity is on the order of 0.05 mΩ cm. These

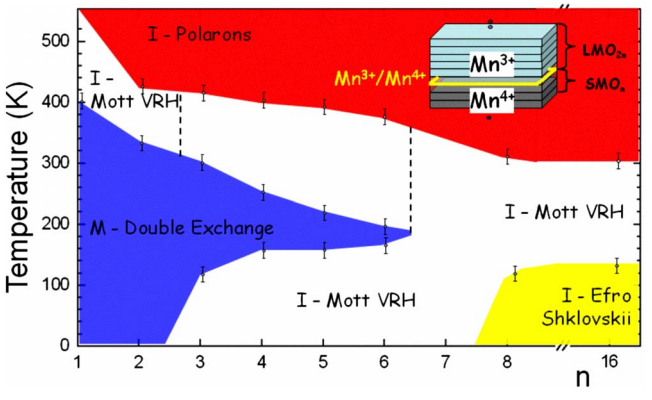

FIG. 1. (Color online) The cartoon summarizes all the different transport regimes obtained changing n (see text). M stands for metal, I for insulator, and VRH for variable range hopping.

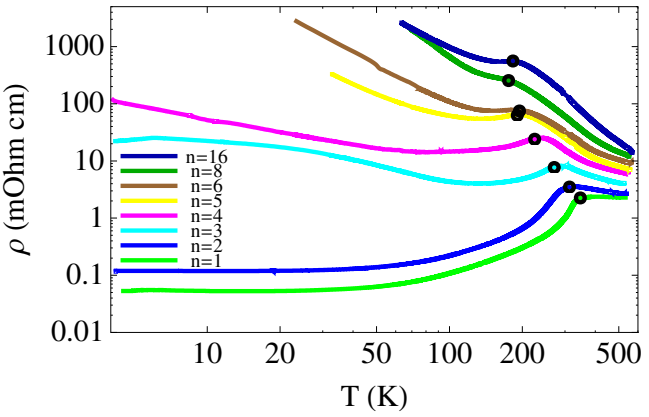

FIG. 2. (Color online) The measured resistivity as a function of temperature for several values of n. Going from bottom to top n increases assuming the values $n=1,2,3,4,5,6,8,16$. The circles mark the experimental Curie temperatures which are always very close to T_{MI}.

values are among the lowest values reported for $La_{1-x}Sr_xMnO_3$ films, signaling low disorder.[7] The high-temperature resistivity for $n=1$ is also suggesting low disorder. It is, indeed, similar to that observed in the cleanest $La_{1-x}Sr_xMnO_3$ films where the metal-insulator (MI) transition is slight. Finally, for the SL with $n>1$ at temperatures higher than 400 K, an activated behavior is clearly present, with an activation energy slightly increasing with n in the range of 300–700 K. These values are much lower than those observed in manganite films with similar T_{MI},[8] again indicating a low amount of disorder in these layered systems.

III. RESISTIVITY VERSUS TEMPERATURE FOR DIFFERENT SLs: FITTING PROCEDURE

In Fig. 2, the resistivity of the $(SMO)_n/(LMO)_{2n}$ samples with $n=1-16$ is shown. Small circles mark the Curie temperature as measured by superconducting quantum interference device (SQUID) magnetometry.[6] The sample with $n=8$ exhibits insulating $(d\rho/dT<0)$ behavior at all temperatures, with a rounding of the $\rho(T)$ curve around 250 K. For $n=6$, the behavior is insulating at low and high temperatures, while a metallicke regime $(d\rho/dT>0)$ appears at intermediate temperatures below the maximum, marking the MI transition temperature T_{MI}.

The $n=3$ sample is on the verge of a new behavior since, at very low T, the resistivity increases as a function of temperature. For $n=2$, the low-temperature resistivity is metallic indicating that the system has undergone a MI transition. The charge transfer through the interfaces becomes predominant making the system similar to A-site alloy $La_{1-x}Sr_xMnO_3$ films. This mechanism becomes very effective in the case $n=1$, where the thickness of the SMO layers is just one unit cell. With decreasing n, the metallic behavior below T_{MI} involves larger temperature ranges and T_{MI} increases. Similar results have been obtained also in other SLs, even though the transport properties were not investigated over as wide a range of temperatures and n values.[5]

TABLE I. The values of the parameters obtained by fitting the resistivity in different temperature ranges (see the text). MP is the metallic phase, M-VRH (HT) is the Mott variable range hopping above the Curie temperature, M-VRH (LT) is the same below the Curie temperature, ES-VRH is the Efros-Shklovskii variable range hopping, and PP is the polaronic phase. ρ_0 is measured in mΩ cm.

	MP		M-VRH (HT) $\beta=0.25$	M-VRH (LT) $\beta=0.25$	ES-VRH $\beta=0.5$	PP $\beta=1.0$
n	α	ρ_0	T_0 (K)	T_0 (K)	T_0 (K)	T_0 (K)
1	2.44	0.052	62			
2	2.60	0.119	2.2×10^4			266
3						499
4				1.2×10^3		499
5				1.2×10^5		603
6				3.1×10^5		661
8			2×10^6		3.2×10^3	1070
16			2×10^4		1.5×10^3	1429

The transport properties have been analyzed systematically in several ranges of T and n. We have fitted the $\rho(T)$ curves by using the formulas $(\rho-\rho_0)\sim T^\alpha$ and $\rho(T)\sim\exp(T_0/T)^\beta$ for the metallic and insulating behaviors, respectively. The parameters α, β, T_0, and ρ_0 were obtained by a best-fit procedure choosing different temperature ranges and varying their amplitudes systematically in order to have stable results for the fitting parameters. In Table I we report the values of α, β, ρ_0, and T_0 for different n.

IV. MODEL

In order to analyze the results, we adopted a recently proposed model where the layers of La^{3+} are considered to be donor ions in a lattice of SMO with the doped electrons going into the e_g states on the Mn sites and bound to the La^{3+} layer via an attractive Coulomb potential.[9,10] All these interactions give rise to an effective potential that, for the sake of simplicity, we assume to be a simple attractive barrier corresponding to the La^{3+} sites. We also included the coupling to local phonons (Holstein model) that is considered very important in manganites[9] and, therefore, the model Hamiltonian becomes

$$H=-t\sum_{\langle i,j\rangle}\frac{S_0^{i,j}+1/2}{2S+1}c_i^+c_j+\omega_0\sum_i a_i^+a_i+g\omega_0\sum_i n_i(a_i+a_i^+)$$
$$-J\sum_{\langle i,j\rangle}\vec{S}_i\cdot\vec{S}_j+\sum_i\varepsilon_i c_i^+c_i. \quad (1)$$

Here t is the transfer integral between nearest neighbors, $S_0^{i,j}$ is the total spin of the subsystem consisting of two localized spins on two neighbor sites and the conduction electron, S is the spin of the core states, and $c_i^\dagger$ (c_i) creates (destroys) an electron with spin parallel to the ionic spin at the ith site. The first term of the Hamiltonian describes the double-exchange mechanism in the limit where the intra-atomic exchange in-

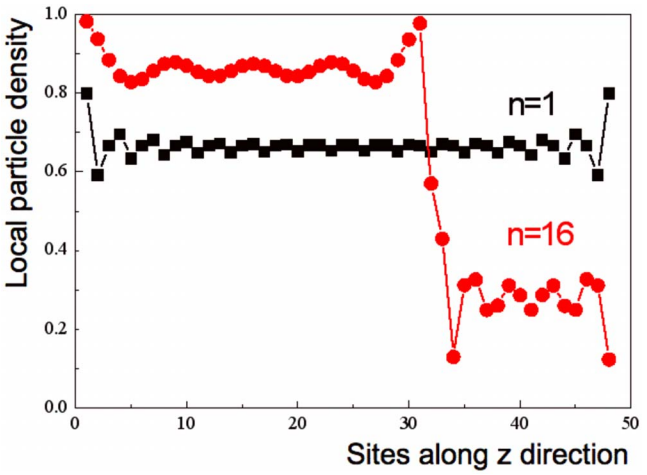

FIG. 3. (Color online) Particle density, derived from the model discussed in the text, as a function of the site position along the growth direction z of the SL: $n=1$ (black squares) and $n=16$ (red circles). The electron-phonon coupling has been chosen to be in the range of intermediate strength (see Ref. 11).

tegral is far larger than the transfer integral t. Furthermore, in Eq. (1), ω_0 denotes the frequency of the local optical-phonon mode, $a_i^\dagger$ (a_i) is the creation (annihilation) phonon operator at the site i, the dimensionless parameter g indicates the strength of the electron-phonon interaction in the Holstein model, and J represents the antiferromagnetic superexchange coupling between two neighbor t_{2g} spins. Finally, ε_i controls the attractive barrier corresponding to the La^{3+} sites. Treating the model within the inhomogeneous mean-field approach developed in Ref. 11, we are able to calculate the local charge density for different n obtaining a simple scenario for interpreting the experimental results (Fig. 3). It is worth mentioning that the used method[11] has been successfully tested for bulk and films of different doped A-site alloy manganites (at different hole dopings x ranging from $0<x<0.5$) and extended here to the SL. In this doping range the results of our approach are fully consistent with those obtained within the dynamical mean-field theory (DMFT) with the advantage of a less demanding computational effort.

V. DISCUSSION OF THE DIFFERENT TEMPERATURE REGIMES

A. Temperatures below T_{MI} for $n=1,2$

In this case the sample resistivities are metallic down to the lowest temperatures. The fitting procedures $(\rho-\rho_0)\sim T^\alpha$ provide α value of 2.44 (2.60) and a ρ_0 value of 0.052 (0.119) mΩ cm for $n=1$ (2). This result is in full agreement with the model results that, as shown in Fig. 3 for $n=1$, predicts a local hole doping nearly equal to the SL nominal doping $c=1/3$. There are only very small density oscillations related to the presence of interfaces. Actually, due to a local mixed-valence state brought about by the transfer of e_g electrons from LMO into SMO, a ferromagnetic metallic region of one or two unit cells is stabilized at a $(SMO)_n/(LMO)_{2n}$ interface.[9] In the cases $n=1$ and $n=2$, the layers are so thin that the double-exchange mechanism becomes predominant giving rise to the low-temperature metallic behavior. The e_g electrons hardly see the spatial separation between SMO and LMO layers whose electronic bands are strongly hybridized. These results explain the strong similarity of the transport properties with those of films with $x=0.3$. Actually, the system can be described qualitatively by an effective hopping amplitude t_{eff}. Then the transport properties are controlled by the ratio between the relatively small disorder energy within the SMO and LMO layers and the effective amplitude t_{eff}. In the low-temperature metallic phases, the effects of disorder are finite but small (see, for example, the low value of ρ_0 compared with that of $La_{1-x}Sr_xMnO_3$ films). The difference in ρ_0 between $n=1$ and $n=2$ can be simply understood if one takes into account that t_{eff} decreases for $n=2$.

B. Temperatures below T_{MI} for $n=3,4,5,6$

In these cases the resistivity is no longer metallic except for a small temperature range just below T_{MI}. Due to the smallness of this metallic region the fitting procedure is not able to provide reliable results. On the other hand the low-temperature resistivity presents an insulating behavior whose best fit is obtained with β values close to 0.25 and T_0 values of 1.24×10^3, 11.85×10^4, and 31.22×10^4 K for $n=4$, 5, and 6, respectively. This behavior is typically associated with the Mott variable range hopping (M-VRH) regime $\rho(T)\sim\exp(T_0/T)^{0.25}$.[12,13] The crossover from metallic to M-VRH behavior is observed at $n=3$ where the resistivity shows a further decrease at very low temperature, typical of the MI transition.

The insulating regime becomes stable at low temperature beginning with $n=3$. It is worth noticing that, for $n=3$, the size of SMO layers is larger than or on the same order of magnitude as the Thomas-Fermi screening length for manganites.[9] Actually, the charge transfer through the interfaces is reduced, implying that t_{eff} becomes very small. Therefore the effects due to disorder are amplified and a MI transition takes place at low temperature. At the same time, ferromagnetism becomes a tiny interface effect opening the possibility for more complicated magnetic orderings within the layers. If one considers the density of states at the Fermi level $N(E_F)$ of the bulk alloy at $x=0.3$ [$N(E_F)\simeq4\times10^{28}$ m^3 eV], the localization length ξ_L can be extracted by the M-VRH law $\xi_L=[18/k_BT_0N(E_F)]^{1/3}$, with k_B as Boltzmann constant. For $n=3$, one gets $\xi_L\simeq1.83$ nm; for $n=4$, $\xi_L\simeq1.65$ nm.[5] Both values are larger than the lattice parameters of manganites. In the case of $n=5$, however, $\xi_L\simeq0.36$ nm, i.e., on the same order as Mn-O-Mn bond distance. Finally, for $n=6$, $\xi_L\simeq0.26$ nm that is on the same order of magnitude as the distance between the manganese and the oxygen atoms. The case $n=6$ represents a limit for the M-VRH mechanism since the localization length has to be equal to or larger than the minimum hopping length.[13] Actually, if one tries to describe the low-temperature resistivity of the samples with $n=8$ by using the M-VRH, one does not find an accurate fit and the value of ξ_L is smaller than the Mn-O distance. This is a clear indication that, in the case $n=8$, the transport mechanism is different.

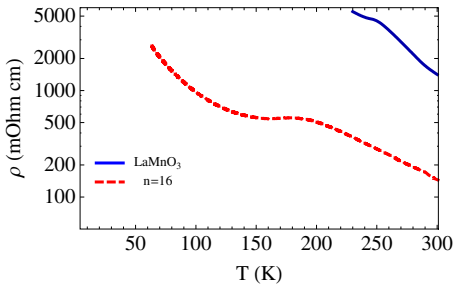

FIG. 4. (Color online) The experimental resistivity of the bilayer, corresponding to $n=16$, (dashed red) is compared with that of a LMO film with very low resistivity (full blue).

C. Temperatures above T_{MI} for n up to 6

The best fit for the resistivity curve at $n=1$, in the range from T_{MI} to 600 K, gives a M-VRH behavior with $\beta=0.25$ and T_0 on the order of 62 K. For $n=2$, both M-VRH and activated hopping are observed together. From T_{MI} to about 400 K, M-VRH mechanism is still active with very large T_0 (on the order of 20 000 K), and for higher temperatures $\rho(T)$ curve can, instead, be fitted by an activated mechanism ($\beta=1$) that can be ascribed to polaron formation with T_0 on the order of 300 K. Such complex insulating behavior can be understood as follows. Just below T_{MI} the observed metallic state is favored by an increase in ferromagnetic fluctuations.[5] With increasing temperature, the ferromagnetic order is weakened; therefore, the hopping of e_g electrons becomes less effective due to the reduction in the double exchange mechanism. At temperatures higher than T_{MI}, this gives rise again to a disorder-induced MI transition (Mott type). For both the cases of $n=1$ and $n=2$, the ratio between the localization length ξ_L and the Mn-O-Mn bonding distance is larger than 1 (specifically, it is 11.26 and 1.64 for $n=1$ and $n=2$, respectively) and, therefore, the hopping to nearest neighbors is highly probable. The M-VRH mechanism needs a boson in order to become active.[13] At high temperatures, local phonons, responsible for lattice distortions in $La_{1-x}Sr_xMnO_3$ samples,[14] are natural candidates for this purpose. With a further increase in temperature, the hopping process is limited only to nearest neighbors by the interaction with optical phonons because of the formation of polaronic quasiparticles with larger effective masses. Then the crossover from M-VRH to polaronic insulator occurs at a temperature around 400 K with not much large activation energies. The slight increase in T_0 with n, linked to the polaronic binding energy, can be taken as a sign of the cooperative role of disorder and electron-phonon coupling. For $n>2$ a similar behavior is observed with larger polaron binding energies (Table I), even if the M-VRH regime is not well supported by the fitting procedures.

D. Transport properties for $n=8$ and 16

In Fig. 4, the experimental $\rho(T)$ curve of the $n=16$ (bilayer) sample is shown. In the range between 4.2 and 130 K, the experimental curves of the samples with $n=8$ and $n=16$ are best fitted by $\rho(T)\sim\exp(T_0/T)^{\beta}$ with $\beta=0.5$ with $T_0\simeq 1000$ K. This law is traceable back to the Efros-Shklovskii variable range hopping (ES-VRH) mechanism.[13] This behavior is due not only to the presence of disorder but also to the role of the Coulomb interaction that becomes more effective since the screening is weaker due to a lower carrier density. Generally, the ES-VRH behavior undergoes a crossover to the usual M-VRH law with the temperature. Indeed, the experimental curves of our samples with $n=8$ and 16 are well fitted by the M-VRH law in the temperature range between 150 and 230 K. The crossover to the polaronic insulator takes places at larger T on the order of 300 K (typical crossover polaronic temperature in many manganite systems). In addition to the lower crossover temperature, there is a larger polaronic activation energy ($T_0=1000$ K) in comparison with samples with smaller n.

In the case of the bilayer ($n=16$), one would expect that the effect of charge transfer through the interface is almost negligible involving only a few unit cells. Since the resistivity is measured on top of the LMO layer, one would expect very high values of the resistivity since LMO is a Mott-Hubbard insulator ($SrMnO_3$ is also very insulating). Surprisingly, the measured resistivity of the sample with $n=16$, however, is much smaller than that measured on a film of $LaMnO_3$ (see Fig. 4) grown under similar conditions.[4]

In order to investigate this issue, again we have used the model of Eq. (1). For intermediate strength of the electron-phonon coupling,[13] a phase of localized polarons with antiferromagnetic ordering becomes stable within the layers, while ferromagnetism takes place at the interface. In the case of the bilayer, this implies that, neglecting the effect of disorder, the effective hopping within the layer is smaller than that at the interface. This induces a redistribution of the charge throughout all the system. The spatial particle density along the growth direction is shown in Fig. 3. Using realistic parameters,[15] the SMO layer can have an average particle density of order 0.25, while the LMO layer has an average particle density of order 0.875. The main effect is that, through the interface, an effective doping is introduced in the overall system. Since the layers are quite large and the contacts are on LMO, the experimental resistance is roughly given by the parallel combination of the resistances of the two layers. Since the resistivity of $La_{1-x}Sr_xMnO_3$ at a hole doping $x=0.125$ is much smaller than that at $x=0.75$,[14] the main contribution to the overall resistance comes from the LMO layer with an effective density about $x=0.125$.[16] This explains why the measured resistivity is much lower than that of LMO films. A similar behavior is clearly present also for $n=8$, where the thickness of LMO and SMO layers is still sizeable. It is worth noticing that this effect could be stabilized by a small reduction in the in-plane lattice parameters in the bilayer with respect to that observed in the single film.

VI. SUMMARY

We have analyzed the transport properties of $(SMO)_n/(LMO)_{2n}$ SL over a wide range of temperatures by changing n and keeping the total thickness fixed. By using

best-fitting procedures we have identified different transport regimes which can be related to different effective dopings induced by the interfaces. The charge transfer throughout the interface is relevant even in the case of a single interface and extends quite far from the interface.

ACKNOWLEDGMENTS

We acknowledge D. G. Schlom and P. Schiffer for discussing the experimental data and A. Mishchenko for a critical reading of the paper.

[1] A. Ohtomo and H. Y. Hwang, Nature (London) **419**, 378 (2002).
[2] S. Okamoto and A. J. Millis, Nature (London) **428**, 630 (2004).
[3] A. Ohtomo and H. Y. Hwang, Nature (London) **427**, 423 (2004); S. Thiel, G. Hammerl, A. Schmehl, C. W. Schneider, and J. Mannhart, Science **313**, 1942 (2006); N. Reyren, *ibid.* **317**, 1196 (2007).
[4] T. Koida, M. Lippmaa, T. Fukumura, K. Itaka, Y. Matsumoto, M. Kawasaki, and H. Koinuma, Phys. Rev. B **66**, 144418 (2002); H. Yamada, M. Kawasaki, T. Lottermoser, T. Arima, and Y. Tokura, Appl. Phys. Lett. **89**, 052506 (2006).
[5] A. Bhattacharya, S. J. May, S. G. E. te Velthuis, M. Warusawithana, X. Zhai, B. Jiang, J. M. Zuo, M. R. Fitzsimmons, S. D. Bader, and J. N. Eckstein, Phys. Rev. Lett. **100**, 257203 (2008); S. Smadici, Peter Abbamonte, Anand Bhattacharya, Xiaofang Zhai, Bin Jiang, Andrivo Rusydi, James N. Eckstein, Samuel D. Bader, and Jian-Min Zuo, *ibid.* **99**, 196404 (2007).
[6] C. Adamo, X. Ke, P. Schiffer, A. Soukiassian, M. Warusawithana, L. Maritato, and D. G. Schlom, Appl. Phys. Lett. **92**, 112508 (2008).
[7] S. Mercone, C. A. Perroni, V. Cataudella, C. Adamo, M. Angeloni, C. Aruta, G. De Filippis, F. Miletto, A. Oropallo, P. Perna, Y. Petrov, U. S. di Uccio, and L. Maritato, Phys. Rev. B **71**, 064415 (2005).
[8] P. Orgiani, C. Adamo, C. Barone, A. Galdi, A. Yu. Petrov, D. G. Schlom, and L. Maritato, Phys. Rev. B **76**, 012404 (2007).
[9] C. Lin, S. Okamoto, and A. J. Millis, Phys. Rev. B **73**, 041104(R) (2006); C. Lin and A. J. Millis, Phys. Rev. B **78**, 184405 (2008).
[10] I. González, S. Okamoto, S. Yunoki, A. Moreo, and E. Dagotto, J. Phys.: Condens. Matter **20**, 264002 (2008).
[11] C. A. Perroni, V. Cataudella, G. De Filippis, G. Iadonisi, V. Marigliano Ramaglia, and F. Ventriglia, Phys. Rev. B **68**, 224424 (2003); C. A. Perroni, G. De Filippis, V. Cataudella, and G. Iadonisi, *ibid.* **64**, 144302 (2001).
[12] N. F. Mott, *Metal-insulator Transitions*, 2nd ed. (Taylor & Francis, London, 1990).
[13] J. M. D. Coey, M. Viret, L. Ranno, and K. Ounadjela, Phys. Rev. Lett. **75**, 3910 (1995).
[14] E. Dagotto, *Nanoscale Phase Separation and Colossal Magnetoresistance* (Springer, New York, 2003).
[15] Polaron binding energy larger or on the same order of the energy barrier height (in calculations we used a value of $0.6t$).
[16] A. Neifel'd, V. E. Arkhipov, N. A. Tumalevich, and Ya. M. Mukovskii, JETP Lett. **74**, 556 (2001); see the strong similarity of the bilayer resistivity with that of LSMO films at $x=0.125$.